Articles in PresS. Am J Physiol Cell Physiol (July 30, 2003). 10.1152/ajpcell.00179.2003

Distribution and functional properties of human KCNH8 (Elk1) potassium channels.

Anruo Zou, Zhixin Lin, Margaret Humble, Christopher D. Creech, P. Kay Wagoner, Douglas Krafte, Timothy J. Jegla and Alan D. Wickenden[1]

Icagen Inc., 4222 Emperor Boulevard, Durham, North Carolina 27703, USA.

Running title: Distribution and function of human KCNH8.

[1] Address for Correspondence:
Alan D. Wickenden PhD.,
Icagen Inc.,
4222 Emperor Boulevard,
Durham, NC 27703, USA
e-mail: awickenden@icagen.com

Abstract.

The Elk subfamily of the Eag potassium channel gene family is represented in mammals by three genes that are highly conserved between humans and rodents. Here we report the distribution and functional properties of a member of the human Elk potassium channel gene family, KCNH8. Quantitative RT-PCR analysis of mRNA expression patterns showed that KCNH8, along with the other Elk family genes, KCNH3 and KCNH4, are primarily expressed in the human nervous system. KCNH8 was expressed at high levels and the distribution showed substantial overlap with KCNH3. In *Xenopus* oocytes, KCNH8 gives rise to slowly activating, voltage-dependent potassium currents that open at hyperpolarized potentials (half maximal activation occurred at -62mV). Co-expression of KCNH8 with dominant negative KCNH8, KCNH3 and KCNH4 subunits lead to suppression of the KCNH8 currents, suggesting that Elk channels can form heteromultimers. Similar experiments imply that KCNH8 subunits are not able to form heteromultimers with Eag, Erg or Kv family potassium channels.

Key words: Potassium Channel, Elk, KCNH8, electrophysiology.

Introduction.

Several important families of potassium channel genes were originally discovered in *Drosophila* through the characterization of mutations that caused hyperexcitability. These include the voltage-gated potassium channels (Kv), large conductance calcium-activated potassium channels (BK), and Eag family potassium channels (Papazian *et al*., 1987; Warmke *et al*., 1991; Atkinson *et al*., 1991). The Eag potassium channel gene family derives its name from the *Drosophila* behavioral mutant ether-à-go-go, which exhibits abnormal neuromuscular transmission (Ganetzky and Wu, 1983). Ether-à-go-go was found to have mutations in a novel potassium channel gene that is distantly related to both voltage-gated potassium channels and cyclic nucleotide-gated channels (Warmke *et al*., 1991). A combination of genetic analysis, homology screening and database mining has shown that the Eag gene represents a family of potassium channel genes conserved between *Drosophila* and mammals (Warmke and Ganetzky, 1994; Titus *et al*., 1997; Shi *et al*, 1998, Engeland *et al*., 1998, Ganetzky *et al*., 1999). These Eag family channels share substantial sequence homology in a region of approximately 700 amino acids extending from the N-terminus through a canonical voltage-gated potassium channel motif of 6 transmembrane domains and a potassium channel pore, to a C-terminal region with a cyclic nucleotide binding domain. It has more recently been shown that most Eag family channels also contain an N-terminal PAS domain (Morais Cabral *et al*., 1998). Because of the structural homology to voltage-gated potassium channels, it is very likely that members of the Eag family channels function as tetramers. This likely structure leaves open the possibility that Eag family channels function as heterotetramers in at least some situations as is the case for several other potassium channel families. Cyclic

nucleotides are not necessary for channel activity like they are for cyclic nucleotide-gated channels (Robertson *et al*., 1996). Although the role of cyclic nucleotides in Eag channel gating has not been extensively studied, it is possible that cyclic nucleotides play a subtle role in Eag channel gating like they do for the structurally-related hyperpolarization-activated cation channels from the HCN gene family (Santoro and Tibbs, 1999).

The Eag family consists of three closely related subfamilies of genes defined by sequence homology, Eag, Erg (**e**ther-à-go-go **r**elated **g**ene) and Elk (**e**ther-à-go-go-**l**ike **k** channel). Each of the three subfamilies is defined by the high degree of homology shared among members in the conserved region described above (60-80+% amino acid identity). A somewhat lower level of homology is shared between subfamilies (approximately 40% amino acid identity). All three subfamilies are conserved between *Drosophila* and mammals, suggesting an early origin in metazoan evolution. The Elk subfamily of potassium channels was first discovered in *Drosophila* based on homology to the *Drosophila* Eag potassium channel (Warmke and Ganetzky, 1994). Three distinct mammalian Elk potassium channel genes have since been identified (Shi *et al*., 1998, Engeland *et al*., 1998, Miyake *et al*., 1999). There has been some level of confusion generated in the naming of these Elk genes because the same names were given to distinct genes in two of these publications. In this paper we will refer to the Elk gene presented in Shi *et al*. (1998) as KCNH8. The gene presented as Elk1 in Engeland *et al*. (1998) and as BEC2 in Miyake *et al*. (1999) is referred to as KCNH4, and the gene presented as Elk2 in Engeland *et al*. (1998) and BEC1 in Miyake *et al*. (1999) is referred to as KCNH3. Here we show human KCNH8 is widely expressed in the human central nervous system and appears to overlap the distribution of human KCNH3 and KCNH4,

which are also predominantly expressed in the nervous system. Because Elk channels are likely to function as tetramers, the overlapping distribution raises the possibility that heteromultimeric Elk channels may be functionally relevant *in vivo.* Therefore, we investigated the possibility that Elk channels can form heterotetramers through the coexpression of wild-type (WT) and dominant-negative (DN) Elk family subunits. We report here that distinct Elk channel subunits can coassemble with each other, but that they likely do not coassemble with Eag and Erg family subunits.

Methods.

Cloning

The human KCNH8 gene was cloned using a combination of degenerate PCR and RACE techniques, using a partial genomic sequence and knowledge of conserved Elk family motifs. The complete KCNH8 PCR fragment was TA-cloned and several clones were sequenced completely to establish a consensus sequence and to identify a mutation-free clone. The final KCNH8 cDNA was identical to accession number AY053503. Human KCNH3, KCNH4, KCNH6 (Eag2), KCNH7 (Erg3) and KCNB1 (Kv2.1) genes were cloned from human brain cDNA using similar PCR strategies. The KCNH3 and KCNH4 clones encode proteins identical to those published by Miyake *et al*., 1999 (Genbank accession numbers BA83590 and BA83592). The KCNH6, KCNH7 and KCNB1 clones encode proteins identical to Genbank accession numbers AF032897, AF418206, L02840 (Ikeda *et al*., 1992), respectively. Clones were moved to the pOX vector (Jegla and Salkoff, 1997) for expression in *Xenopus* oocytes.

Dominant negative subunits of human KCNH8, KCNH3 and KCNH4 were constructed using the Quickchange site-directed mutagenesis kit (Stratagene). Briefly, the GFG amino acid sequence contained in the pore motif of each channel was replaced with the amino acid sequence AAA (Kuzhikandathil and Oxford, 2000). Sequences of clones were confirmed to ensure incorporation of the intended mutations and absence of second-site mutations.

Phylogenetic Analysis

Amino acid sequences used in the phylogenetic analysis were limited to a region stretching from the N-terminus to the C-terminal side of the cNBD and alignments were produced using the CLUSTALW algorithm in Megalign (DNASTAR). Phylogenetic trees of Eag family amino acid sequences were built using MEGA2.1 (Kumar *et al*., 2001). The analysis shown in Figure 2 was conducted using the minimum evolution algorithm with poisson correction and pairwise deletion of gaps. 1000 bootstrap replications were used to test the phylogeny. Accession numbers and references for sequences not described above are: rat Kcnh3, AJ007627, Engeland *et al*., 1998; rat Kcnh4, AJ007628, Engeland *et al*., 1998; mouse Kcnh8, AK048629; mouse Kcnh3, AF012868, Trudeau *et al*., 1999; mouse Kcnh4, XM_204529; human KCNH2 (hErg1), U04270, Warmke and Ganetzky, 1994; mouse Kcnh2 (mErg1), AF012868, London *et al*., 1997; mouse Kcnh6 (mErg2), mouse genome draft, Waterston *et al*., 2002; mouse Kcnh7 (mErg3), XM_130310; rat Kcnh2 (rErg1), Z96106, Bauer *et al*., 1998; human KCNH6 (hErg2), AF311913; rat Kcnh6 (rErg2), AF016192, Shi *et al*., 1997; rat Kcnh7 (rErg3), AF016191, Shi *et al*., 1997; human KCNH1 (hEag1), AJ001366, Occhiodorro *et al*., 1998; mouse Kcnh1 (mEag1), U04294, Warmke and Ganetzky, 1994; mouse Kcnh5 (mEag2), AK032438; rat Kcnh1 (rEag1), Z34264, Ludwig *et al*., 1994; rat Kcnh5 (rEag2), AF185637, Saganich *et al*., 1998; drosophila Eag, M61157, Warmke *et al*., 1991; drosophila Elk, U04246, Warmke and Ganetzky, 1994; drosophila Erg, U42204, Titus *et al*., 1997; c.elegans Eag, AF130443, Weinshenker *et al*., 1999; c.elegans Erg, AF257518; Reiner *et al*., 1999; c.briggsae Eag and c.briggsae Erg, C. Briggsae genome draft assembly, Sanger Institute and Genome Sequencing Center, Washington University,

St. Louis, MO; Anopheles gambiae sequences, Ensembl genome server and Holt *et al*., 2002.

Real Time RT-PCR Analysis

Total RNA and polyA$^+$ mRNA samples from various human tissues were obtained from Clontech and cDNA synthesis was performed by standard oligo dT priming methods using PowerScript reverse transcriptase (Clontech). Total RNA samples were DNAse I treated prior to use. All samples were treated with RNAse H prior to amplification. Parallel reactions for each of the RNA samples were run in the absence of PowerScript RT to serve as controls for contamination during subsequent amplification.

The expression patterns of the human Elk genes was determined by real time quantitative PCR techniques (Heid *et al*., 1996) using the ABI prism 7900HT Sequence Detection System (Applied Biosystems). Primers and TaqMan probes for each Elk gene and a reference housekeeping gene (RS9, accession number NM_001013) were designed using Primer Express 2.0 (Applied Biosystems) and purchased from Integrated DNA Technologies. Taqman probes were labeled on the 5' end with a fluorescent reporter dye (FAM; 6-carbosy-fluorescein) and on the 3' end with a quencher dye (BH-1, black hole). Amplicons were designed to span intron/exon boundaries to minimize contamination from genomic DNA and were shorter than 150 bp to allow for efficient amplification. The primers and probes used for each gene were:

KCNH8: GCTTTGCAGGCCATCTACTTTG (+), GGTCTTGATCACTTGGTCCTTAA (-), TTTCCCAAGAATAGCCAGCACCATGCT (probe);

KCNH3: CGAGGCAAGGAACACAGACA (+), CACAGCCTGGCGAAGTGA (-), AGGTGCTGCAGATGCGGGAAGGA (probe);

KCNH4: CCAACGAGTTACTGCGTGACTTC (+), TGCAGGATCTCCCGATTCA (-), CGAGCTGAGAGCTGACATTGCTATGCAC (probe);

RS9 CGCCAGCGCCATATCAG (+), CGATGTGCTTCTGGGAATCC (-), AGCAGGTGGTGAACATCCCGTCCTTC (probe).

All amplifications were preceded by steps to 50°C for 2 minutes and then 95°C for 10 minutes. 40 two-step amplification cycles of 95°C for 15 seconds and 60°C for 1 minute were used to generate the data. Reactions were performed in 20μl using Taqman Universal Master Mix (Perkin Elmer), 300nM each primer and 200nM probe. Quantification of gene expression in the sample RNAs was achieved by comparing the threshold cycle (C_t) values for each sample to a standard curve of C_t vs. copy number (Heid *et al.*, 1996). Control plasmids for standard curve generation were designed for each primer/probe set and quantified using OD_{260}. Copy numbers were determined using the molecular weight of each plasmid, and samples containing 10-10^8 copies were used to generate standard curves. Copy numbers in experimental samples were determined using the equation Log copy number =(Ct-I)/S, where Ct is the threshold cycle value of the sample, I is the intercept and S is the slope of a linear fit of the standard curve data. To allow for comparisons across tissues, the results for each RNA sample were then normalized by dividing the copy numbers obtained for each Elk gene by the copy number obtained for the reference gene RS9. All assays were performed in duplicate and the average values are reported.

Functional Expression in *Xenopus* oocytes.

Capped cRNAs were prepared by run-off transcription with T3 RNA polymerase using the mMessage mMachine kit (Ambion, Austin, TX, USA) and diluted in RNase-free ddH_2O to desired concentrations before injection. Mature *Xenopus* oocytes were prepared for injection as described in Wei *et al.*, 1990. Briefly, X. laevis (Nasco, Ft. Atkinson, Wisc., USA) were anesthetized by immersion in Tricaine solution (0.2% w/v; Sigma Chemical Co., St. Louis, MO, USA). Ovarian lobes were removed through a small incision in the abdominal wall. Oocytes were freed from ovarian lobes by gentle mechanical agitation in Ca^{2+} free ND-96 solution (96 mM NaCl, 2 mM KCl, 1 mM $MgCl_2$, 5 mM HEPES, pH 7.5 with NaOH) containing 1.5mg ml^{-1} collagenase (type 1A, Sigma Chemical Co., St. Louis, MO, USA) for 45-60 min. Oocytes were stored overnight in ND96 supplemented with 1.8mM $CaCl_2$, 100 U/ml penicillin, 100 µg/ml streptomycin, and 2.5 mM sodium pyruvate. Oocytes were injected with 55nl cRNA (0.1 – 1 ng/nl) and incubated at 18°C for 1-5 d prior to recording.

Functional properties of KCNH8.

Human KCNH8 currents in *Xenopus* oocytes were recorded 2-5 days post injection using the two electrode voltage-clamp techique. Microelectrodes were filled with 3M KCl and had tip resistances of approximately 1MΩ. During recording, oocytes were continually perfused with either regular ND96 solution (composition as described above) or elevated potassium ND96 solution (hi-K^+ ND96: 78 mM NaCl, 20 mM KCl, 1 mM $MgCl_2$, 5 mM HEPES, 0.1mM $CaCl_2$, pH 7.5 with NaOH). All recordings were made at room temperature (22 - 24 °C) using a Dagan TEV-200A voltage-clamp amplifier. Data collection and analysis were performed using pCLAMP software (Axon

Instruments, Union City, CA, USA). In order to study the voltage-dependence of activation, the deactivating tail current amplitude was measured at –60 mV following a series of 3 s depolarizing steps (-100 mV to +10 mV in 10 mV increments) from a holding potential of –100 mV. Activation curves were generated by plotting normalized tail current amplitude against the step potential and were fit with a Boltzman distribution according to the following equation:

$$Y = A/\{1+\exp^{[Vm-V½/k]}\} \qquad 1$$

where A is the amplitude of the relationship, $V_{½}$ is the voltage for half activation, V_m is the step potential and k is the slope factor.

In order to describe the timecourse of human KCNH8 activation, currents were elicited with a series of 3 s depolarizing steps from -60 mV to +10 mV in 10 mV increments in regular ND96 from a holding potential of –100 mV and the activation phase was fit with a double exponential function, according to the following equation:

$$I = A_{fast} * (1-\exp(-t/\tau_{fast})) + A_{slow} * (1-\exp(-t/\tau_{slow})) \qquad 2$$

where A_{fast} and A_{slow} are the amplitudes of the fast and slow components and τ_{fast} and τ_{slow} are the activation time constants.

In order to describe the time course of KCNH8 current deactivation, tail currents were elicited by repolarizing to voltages in the range –110mV to –150mV following a 3 s depolarization to +20mV. Tail current decay was best fit with a double exponential function, according to equation 2.

In order to determine the KCNH8 current reversal potential, tail currents were elicited by repolarizing the membrane to potentials in the range –120 mV to –40 or 0 mV in 10 mV increments, following a 3 s voltage step to 20 mV. Measurements of tail currents were made in regular ND96 solution and in hi-K^+ ND96 solution. Reversal potentials were calculated from linear fits of instantaneous tail current amplitude against repolarization potential.

To study the effects of barium, KCNH8 currents were elicited by depolarizing the membrane to 0 mV for 500 ms from a holding potential of -100mV. Ba^{2+} was applied by perfusing the bath with ND96 solution supplemented with $BaCl_2$ at the desired final concentration. Up to six concentrations of Ba^{2+} were tested on each oocyte, with washout after each drug application. Semi-log plots of Ba^{2+} concentration against effect were fit with a logistic function (Origin, MicroCal Software, Northampton, MA) and IC_{50} values determined from the fitted data.

In all studies, linear leak was subtracted using either a P/4 or a P/8 protocol employing voltage steps of the opposite polarity to the test steps from a holding potential of –100mV.

Dominant Negative expression.

The concentration of cRNAs encoding the wild type (WT) ion channels used in the present experiments was empirically determined in order to generate current amplitudes between 1 and 10μA on the day of study (typically 0.1 – 1ng/nl for Elk, Erg and Eag channels and 1pg/nl for KCNB1). cRNA encoding WT human KCNH8, hEag2, hErg3 was co-injected with a fixed amount (0.1 ng/nl) of cRNA encoding a dominant

negative (DN) Elk subunit. KCNH8, Eag or Erg current amplitude was determined in oocytes injected with WT cRNA alone and this was compared with current amplitude in oocytes co-injected with WT and DN cRNAs. In order to determine if co-injection of DN cRNAs could suppress WT ion channel gene expression in a non-specific manner (for example by saturation of translation or protein synthesis), DN cRNAs were co-injected with an unrelated K^+ channel Kv2.1.

Statistics.

All data are expressed as mean ± standard error of the mean (s.e.m) for $n \geq 3$ observations. Statistical significance was determined using a suitable (hetero- or homoscedastic) 2-tailed unpaired t-test. A $P < 0.05$ was considered significant.

Results

Molecular Conservation of KCNH8

Human KCNH8 encodes a protein of 1107 amino acids containing all the key features of an Eag family channel. An alignment of the deduced amino acid sequence of KCNH8 to the rat Kcnh8 ortholog, human KCNH3 and human KCNH4 is shown in Figure 1. The amino acid sequences of human KCNH8 and rat Kcnh8 are over 90% identical, with the vast majority of divergence occurring downstream of a potential cyclic nucleotide binding domain in the C-terminal cytoplasmic region. A very similar pattern of sequence conservation is observed between human and rat KCNH3 and KCNH4 genes, with amino acid identities of 95% and 89% respectively. The amino acid identity shared between Elk family paralogs is much lower at 45-55% across the entire proteins. Conservation is higher (60-70% amino acid identity) when the comparison is limited to a highly conserved region extending from the N-terminal through the cyclic nucleotide-binding domain. Members of the Eag (KCNH1 and KCNH5) and Erg (KCNH2, KCNH6 and KCNH7) channel subfamilies share only 35-44% amino acid identity with Elk subfamily channels over this region, providing a clear molecular definition of an Elk channel subfamily.

A phylogenetic analysis of the Eag potassium channel family is shown in Figure 2. The three gene subfamilies (Eag, Elk and Erg) are clearly defined by three separate branches. Each subfamily is represented by multiple genes in mammals. The mammalian genes group separately from the insect and worm genes in each subfamily, suggesting that the diversification of the Eag, Elk and Erg subfamilies in mammals occurred after the divergence of vertebrates and invertebrates. While insects and worms

have highly conserved Eag family genes, they do not have specific orthologs of the eight mammalian Eag family genes. Interestingly, we did not find Elk orthologs in either the *C. elegans* or *C. briggsae* genomes, suggesting that the Elk subfamily has been lost in nematodes. We could not determine the order of divergence of the three subfamilies from a common ancestor because no two subfamilies consistently grouped together in bootstrap tests of phylogenies.

We assessed the mRNA expression patterns of human Elk channels using the real time quantitative PCR. Comparisons of the expression levels of the genes were facilitated by normalization of the results to standard curves for each gene, and comparisons of expression levels in different tissues were made possible by normalization to the housekeeping gene RS9. We have found RS9 to be a reliable housekeeping gene over a wide range of tissues. The results presented here agree very well with the results of Northern hybridizations performed for each gene (data not shown). All three Elk genes are primarily expressed in the nervous system and are especially prominent in the forebrain (Figure 3). KCNH3 was the predominant Elk gene expressed in the cerebral cortex, hippocampus, amygdala, caudate and nucleus accumbens. Nevertheless, the other Elk genes, KCNH8 and KCNH4, were also expressed in these tissues, suggesting the possibility of coexpression at the cellular level in at least some subpopulations of neurons. KCNH8 and KCNH3 genes were also expressed together in the thalamus, substantia nigra, pons and cerebellum, but in these tissues, the balance of expression level is shifted towards KCNH8. Expression of all three genes was very low in non-neuronal tissues (data not shown). In each case, testis showed the most significant expression at 0.59, 1.13 and 0.11% RS9 for KCNH8,

KCNH3, and KCNH4, respectively. The unique, yet overlapping expression patterns of the human Elk genes suggested to us that both homomultimeric and heteromultimeric Elk channels may be functionally relevant in the human brain.

Functional properties of human KCNH8.

To characterize the biophysical properties of the human KCNH8 gene product, we expressed KCNH8 in *Xenopus* oocytes. As shown in figure 4A, robust, slowly activating currents were routinely recorded from oocytes injected with human KCNH8 cRNA. KCNH8 currents exhibited a small amount of inactivation at test potentials ≥ +10 mV and similar currents were never recorded from uninjected oocytes (data not shown). In regular ND96 solution, KCNH8 outward currents could be resolved at potentials positive to –90mV. However, the true threshold for activation of KCNH8 channels was difficult to determine in regular ND96 solution since the threshold voltage occurred at potentials that were close to E_K under these conditions. In order to study the voltage-dependence of channel activation, deactivating tail current amplitude was measured at –60 mV following a series of 3 s depolarizing steps (-100 mV to +10 mV in 10 mV increments). The KCNH8 activation curve shown by the circles in Figure 4C was constructed by plotting normalized tail current amplitude against the step potential and fitting the data with a Boltzman distribution. These studies confirmed that KCNH8 activated at voltages of above –90mV and, on average, the voltage at which half-maximal activation occurred (V½ act) was –62.4mV ± 1.2 mV (k = 10.7 ± 0.3 mV; n = 10). KCNH8 currents were also recorded in hi-K^+ ND96 solution, as illustrated in figure 4B. Under these conditions, inward currents were observed at voltages between –90mV and –50mV, whereas outward

currents were observed at voltages above –40mV. Repolarization to –60mV following 3 s depolarizing steps (-100 mV to +10 mV in 10 mV increments) elicited inward tail currents. Activation curves generated from these inward tail currents were similar to those generated in normal ND96 solution (threshold for activation = –90mV and V½ act = -68.0 ± 1.2 mV, k = 10.4 ± 0.7 mV; n = 8).

In order to confirm the currents measured were potassium currents, we measured the reversal potential of voltage-activated currents in KCNH8 injected oocytes in normal and elevated extracellular K^+. Currents were elicited by 3 s voltage steps to 20 mV and tail currents were obtained by repolarization to a series of potentials in the range –120 mV to –40 or 0 mV in 10 mV increments. Reversal potentials were calculated from linear fits of instantaneous tail currents (see methods) against repolarization potential. The KCNH8 reversal potentials were calculated as –93 ± 1.5 mV (n = 10) and –44.4 ± 3.0 mV (n = 5) in normal ND96 and in hi K^+ ND96, respectively (figure 4D). These values were plotted against the extracellular K^+ concentration and fitted with a logarithmic regression, yielding a slope of 48 mV per decade. These results indicate that KCNH8 encodes a K^+-selective channel, although the slope value was marginally less than the slope value predicted for a purely K^+ selective channel (58mV per decade, see dashed line in figure 4D).

KCNH8 current activation at voltages between –60 mV and + 10mV (activation time courses could not be accurately fit above +10mV because of inactivation) was fit using an exponential function and two distinct kinetic components were identified. As shown in

Figure 4E, both activation time constants were voltage-dependent. For example, τact_{slow} decreased from 1674 ± 102 ms (n = 12) at –60 mV to 259 ± 29 ms (n = 12) at +10 mV. Similarly, τact_{fast} decreased from 293 ± 19 ms (n = 12) at –60mV to 44.7 ± 3.6 ms (n = 12) at +10mV. In order to describe the time course of KCNH8 current deactivation, tail currents were elicited by repolarizing to voltages in the range –110mV to –150mV following a 3 s depolarization to +20mV and tail current decay was fit with an exponential function. As for activation, deactivation was best described by the sum of two kinetically distinct and voltage dependent components ($\tau deact_{slow}$ and $\tau deact_{fast}$). $\tau deact_{slow}$ increased from 260 ± 25 ms (n =10) at –150 mV to 331 ± 33 ms (n =10) at -110 mV whereas $\tau deact_{fast}$ increased from 28 ± 2.2 ms (n = 10) at –150mV to 65.6 ± 4.4 ms (n = 10) at –110mV (Figure 4F).

In pharmacological experiments, Ba^{2+} inhibited KCNH8 currents with an IC_{50} value of 0.18 ± 0.03 mM (slope = 0.82 ± 0.03, n = 6).

KCNH8 co-assembles with KCNH3 and KCNH4.

Our quantitative PCR data demonstrate that KCNH8 is co-expressed with other members of the Elk family in many brain regions. These data raise the possibility that human KCNH8 may form heteromultimeric channel complexes with human KCNH3 and/or human KCNH4 in the brain. In order to investigate this possibility further we used a dominant negative strategy to determine whether KCNH8 channels are capable of co-assembling with KCNH3 and KCNH4 in the *Xenopus* oocyte expression system. As described in the methods section, wild-type (WT) human KCNH8 cRNA was injected at

a concentration sufficient to generate sub-maximal KCNH8 currents, similar to those shown in Figure 5A. KCNH8 currents were elicited with a series of 3 s depolarizing steps (-100 mV to +40 mV in 10 mV increments) and mean (± S.E.M) current amplitude is plotted against voltage in figure 5E. On average, KCNH8 current amplitude at +40 mV was 6.6 ± 0.34 μA (n = 8) following injection of KCNH8 cRNA alone (Figure 5E). Co-injection of the same amount of WT KCNH8 cRNA with dominant negative (DN) KCNH3 (Figure 5C) or KCNH4 (Figure 5D) resulted in a marked decrease in current amplitude. KCNH8 current amplitude at +40 mV was significantly ($P < 0.05$) reduced from 6.6 ± 0.34 μA (n = 8) in oocytes injected with KCNH8 alone to 2.9 ± 0.6 μA (n = 8) or 1.5 ± 0.1 μA (n = 8) in oocytes injected with either KCNH8/KCNH3-DN or KCNH8/KCNH4-DN, respectively (Figure 5E). Comparable reductions in KCNH8 current amplitude were also observed when oocytes were injected with KCNH8/KCNH8-DN (Figures 5B and 5E). The results of these dominant negative experiments suggest that closely related human Elk family subunits are capable of co-assembling in *Xenopus* oocytes.

Using the same dominant negative strategy, we next sought to determine whether human Elk subunits were also capable of co-assembling with the more distantly related members of the Eag potassium channel family, human KCNH5 (hEag2) and human KCNH7 (hErg3). Mean (± S.E.M) current amplitudes measured in oocytes expressing KCNH5 alone, KCNH5/KCNH3-DN or KCNH5/KCNH4-DN are plotted against voltage in Figure 6A. hElk dominant negative subunits did not reduce KCNH5 current amplitude at any voltage. Peak KCNH5 current amplitude at +40mV was 10.4 ± 0.4 μA (n = 13) in oocytes injected with KCNH5 alone and 10.3 ± 0.4 μA (n = 10) and 10.4 ± 0.5 μA (n =

9) in oocytes injected with KCNH5/KCNH3-DN and hKCNH5/KCNH4-DN, respectively ($P > 0.05$). hElk dominant negative subunits were similarly without effect on KCNH7 currents. Current-voltage relationships for KCNH7 in the absence or presence of hElk dominant negative sub-units are shown in figure 6B. Peak KCNH7 current amplitude was 2.6 ± 0.2 μA ($n = 8$) in oocytes injected with KCNH7 alone and 2.5 ± 0.2 μA ($n = 7$) and 2.4 ± 0.2 μA ($n = 8$) in oocytes injected with KCNH7/KCNH3-DN and hErg3/hKCNH8-DN, respectively ($P > 0.05$). The findings of these studies indicate that hElk family subunits are incapable of co-assembling with more distantly related members of the hEag family in *Xenopus* oocytes. In order to determine if co-injection of dominant negative cRNAs could suppress ion channel gene expression in a non-specific manner, dominant negative hElk constructs were co-injected with an unrelated K^+ channel, human KCNB1 (Kv2.1). At the concentrations used in the present study, hElk dominant negative subunits did not reduce KCNB1 expression (Figure 6C), suggesting that the dominant negative constructs used in the present study did not exert a non-specific inhibitory effect on K^+ channel gene expression.

Discussion

Three distinct mammalian Elk potassium channel genes, KCNH8, KCNH3 and KCNH4, have been identified (Shi *et al*., 1998, Engeland *et al*., 1998, Miyake *et al*., 1999). In the present study we have measured KCNH8 gene expression in the human brain using real-time RT-PCR analysis, and we have characterized the functional properties of the KCNH8 gene product. Our results show that the sequence and structure of the KCNH8 gene is highly conserved between humans and rat. The approximately 90% amino acid identity shared between human and rat KCNH8 is a rather typical level of conservation for ion channel genes, and is seen for human-rodent comparisons of the other Elk subfamily genes.

The *Drosophila* Elk gene provides evidence that the Elk subfamily is conserved in invertebrates, but the level of conservation of biophysical properties is not known because this gene has not yet been heterologously expressed. Interestingly, the Elk family appears to be absent in nematodes. Because two distinct nematode genomes have been sequenced virtually to completion, it is highly unlikely that a nematode Elk gene was missed. Although the majority of ion channel types that are conserved between mammals and *Drosophila* are also found in nematodes, there are other cases similar to this. For instance, voltage-gated sodium channels also appear to be missing in nematodes. Without a clear definition of the physiological role of Elk subfamily channels, it is difficult to speculate why the Elk family is absent in nematodes.

The results presented here and elsewhere suggest that KCNH8, along with KCNH3 and KCNH4, are primarily expressed in the nervous system. Furthermore, in situ hybridization in the rat shows that the Elk genes are expressed almost exclusively in

neurons (Saganich *et al*., 2001). In the human brain, KCNH3 was the predominant Elk gene expressed. KCNH3 has also been shown to be the most abundant Elk gene expressed in the rat brain (Saganich *et al*., 2001). The distribution of human and rat KCNH3 appears to be very similar, with both being highly expressed in many forebrain structures. In contrast, our data shows distinct distributions for the human and rat KCNH8 and KCNH4. In rat, KCNH4 is expressed in many forebrain regions, while KCNH8 is virtually absent (Saganich *et al*., 2001). In humans, almost the opposite appears to be the case, with KCNH8 more highly and widely expressed. Such divergent distributions of human and rat orthologs is not unknown in the ion channel field. Another example of this phenomenon is found in DRASIC, or ASIC3, a pH-sensitive member of the amiloride-sensitive sodium channel gene family. DRASIC appears to be expressed almost exclusively in sensory neurons in rats (Waldmann *et al*., 1997), while its human ortholog (ASIC3) is highly expressed in a wide variety of neuronal and non-neuronal tissues (Babinski *et al*., 1999).

Human KCNH8 currents in *Xenopus* oocytes activate slowly over a hyperpolarized voltage range, exhibit little inactivation near the resting potential, and are inhibited by Ba^{2+}. While slow kinetics, lack of inactivation and Ba^{2+}-sensitivity have also been noted for rat Kcnh8, it is interesting to note that the rat ortholog appears to activate over a more depolarized voltage range (mid-point for activation of rat Kcnh8 was +9.3 mV in the study of Shi *et al*., 1998 compared to –62 mV for human KCNH8 in the present study). This observation was somewhat surprising given the high degree of sequence homology between human and rat KCNH8 genes. The biophysical properties

of human KCNH8 are very similar to those reported for rat Kcnh4 (Engeland *et al*, 1998) and thus it seems likely that these channels serve similar physiological roles. In contrast, human KCNH8 currents exhibit properties that are quite distinct from those reported for KCNH3 currents, that activate at slightly more depolarized potentials and undergo substantial inactivation at depolarized potentials (Engeland *et al*, 1998; Trudeau *et al* ., 1999; Miyake *et al*., 1999; Becchetti et al., 2002). The precise physiological role of Elk channels is not known because so little is known about their modulation and there are currently no pharmacological tools to isolate Elk currents in primary neurons. We can guess from their distribution and biophysical properties that Elk channels likely play a role in modulating the overall excitability of neurons. Their hyperpolarized activation, lack of inactivation near the resting potential and slow kinetics are reminiscent of the M-currents encoded by KCNQ family genes (Wang *et al*., 1998).

As noted above, KCNH3 is the predominant Elk gene expressed in the human central nervous system. This finding suggests that KCNH3 homomultimeric channels may play a significant role in the control of central nervous system excitability. Nevertheless, the other Elk genes, KCNH8 and KCNH4, were also expressed in the human central nervous system, with KCNH8 expression overlapping that of KCNH3 and KCNH4 in some regions. Because Elk channels, like other K^+ channels, are likely to function as tetramers, the overlapping distribution raises the possibility that heteromultimeric Elk channels may exist in many brain regions *in vivo*. We investigated the possibility that Elk channels can form heterotetramers through the coexpression of wild-type and dominant-negative Elk family subunits. Our findings show that dominant negative Elk channel subunits reduce expression of full length Elk but not Eag or Erg

channels. These findings indicate that Elk channel sub-units are able to form heterotetramers with other members of the Elk family but not with members of the Eag or Erg family. Our observations support the findings of Wimmers *et al* (2001), who used a similar dominant negative strategy to demonstrate sub-family selective heterotetramerization among Erg channels subunits.

In conclusion, we have found that KCNH8, along with other Elk family genes, are primarily expressed in the human nervous system. Elk channel subunits can coassemble with each other, but they do not coassemble with Eag and Erg family subunits. Given the overlapping expression of the three human Elk genes and the observation that they can form heteromultimers, it is possible that heteromultimers contribute to native Elk currents in at least some regions of the human brain.

References

Adams MD, Celniker SE, Holt RA, Evans CA, Gocayne JD, Amanatides PG, Scherer SE, Li PW, Hoskins RA, Galle RF, George RA, Lewis SE, Richards S, Ashburner M, Henderson SN, Sutton GG, Wortman JR, Yandell MD, Zhang Q, Chen LX, Brandon RC, Rogers YH, Blazej RG, Champe M, Pfeiffer BD, Wan KH, Doyle C, Baxter EG, Helt G, Nelson CR, Gabor GL, Abril JF, Agbayani A, An HJ, Andrews-Pfannkoch C, Baldwin D, Ballew RM, Basu A, Baxendale J, Bayraktaroglu L, Beasley EM, Beeson KY, Benos PV, Berman BP, Bhandari D, Bolshakov S, Borkova D, Botchan MR, Bouck J, Brokstein P, Brottier P, Burtis KC, Busam DA, Butler H, Cadieu E, Center A, Chandra I, Cherry JM, Cawley S, Dahlke C, Davenport LB, Davies P, de Pablos B, Delcher A, Deng Z, Mays AD, Dew I, Dietz SM, Dodson K, Doup LE, Downes M, Dugan-Rocha S, Dunkov BC, Dunn P, Durbin KJ, Evangelista CC, Ferraz C, Ferriera S, Fleischmann W, Fosler C, Gabrielian AE, Garg NS, Gelbart WM, Glasser K, Glodek A, Gong F, Gorrell JH, Gu Z, Guan P, Harris M, Harris NL, Harvey D, Heiman TJ, Hernandez JR, Houck J, Hostin D, Houston KA, Howland TJ, Wei MH, Ibegwam C, Jalali M, Kalush F, Karpen GH, Ke Z, Kennison JA, Ketchum KA, Kimmel BE, Kodira CD, Kraft C, Kravitz S, Kulp D, Lai Z, Lasko P, Lei Y, Levitsky AA, Li J, Li Z, Liang Y, Lin X, Liu X, Mattei B, McIntosh TC, McLeod MP, McPherson D, Merkulov G, Milshina NV, Mobarry C, Morris J, Moshrefi A, Mount SM, Moy M, Murphy B, Murphy L, Muzny DM, Nelson DL, Nelson DR, Nelson KA, Nixon K, Nusskern DR, Pacleb JM, Palazzolo M, Pittman GS, Pan S, Pollard J, Puri V, Reese MG, Reinert K, Remington K, Saunders RD, Scheeler F, Shen H, Shue BC, Siden-Kiamos I, Simpson M, Skupski MP, Smith T, Spier E, Spradling AC, Stapleton M, Strong R, Sun E, Svirskas R, Tector C, Turner R, Venter E, Wang AH, Wang X, Wang ZY, Wassarman DA, Weinstock GM, Weissenbach J, Williams SM, WoodageT, Worley KC, Wu D, Yang S, Yao QA, Ye J, Yeh RF, Zaveri JS, Zhan M, Zhang G, Zhao Q, Zheng L, Zheng XH, Zhong FN, Zhong W, Zhou X, Zhu S, Zhu X, Smith HO, Gibbs RA, Myers EW, Rubin GM, Venter JC.. The genome sequence of Drosophila melanogaster. *Science* 287 : 2185-2195, 2000.

Atkinson NS, Robertson GA, and Ganetzky, B. A component of calcium-activated potassium channels encoded by the Drosophila slo locus. *Science* 253: 551-555, 1991.

Babinski K, Le KT, and Seguela P. Molecular cloning and regional distribution of a human proton receptor subunit with biphasic functional properties. *J. Neurochem* 72: 51-57, 1999.

Bauer CK, Engeland B, Wulfsen I, Ludwig J, Pongs O, and Schwarz JR. RERG is a molecular correlate of the inward-rectifying K current in clonal rat pituitary cells. *Receptors Channels* 6:19-29, 1998.

Becchetti A, De Fusco M, Crociani O, Cherubini A, Restano-Cassulini R, Lecchi M, Masi A, Arcangeli A, Casari G, Wanke E. The functional properties of the human ether-à-go-go-like (HELK2) K+ channel. *Eur J Neurosci* 16:415-28, 2002.

Engeland B, Neu A, Ludwig J, Roeper J, and Pongs O. Cloning and functional expression of rat ether-à-go-gө like K+ channel genes. *J Physiology*, 513: 647-654, 1998.

Ganetzky B, and Wu CF. Neurogenetic analysis of potassium currents in Drosophila: synergistic effects on neuromuscular transmission in double mutants. *J Neurogenetics* 1: 17-28, 1983.

Ganetzky B, Robertson GA, Wilson GF, Trudeau MC, and Titus SA. The eag family of K+ channels in Drosophila and mammals. *Ann New York Acad Sci* 868:356-369, 1999.

Heid CA, Stevens J, Livak KJ, and Williams PM. Real time quantitative PCR. *Genome Research* 6:986-994, 1996.

Holt RA, Subramanian GM, Halpern A, Sutton GG, Charlab R, Nusskern DR, Wincker P, Clark AG, Ribeiro JM, Wides R, Salzberg SL, Loftus B, Yandell M, Majoros WH, Rusch DB, Lai Z, Kraft CL, Abril JF, Anthouard V, Arensburger P, Atkinson PW, Baden H, de Berardinis V, Baldwin D, Benes V, Biedler J, Blass C, Bolanos R, Boscus D, Barnstead M, Cai S, Center A, Chatuverdi K, Christophides GK, Chrystal MA, Clamp M, Cravchik A, Curwen V, Dana A, Delcher A, Dew I, Evans CA, Flanigan M, Grundschober-Freimoser A, Friedli L, Gu Z, Guan P, Guigo R, Hillenmeyer ME, Hladun SL, Hogan JR, Hong YS, Hoover J, Jaillon O, Ke Z, Kodira C, Kokoza E, Koutsos A, Letunic I, Levitsky A, Liang Y, Lin JJ, Lobo NF, Lopez JR, Malek JA, McIntosh TC, Meister S, Miller J, Mobarry C, Mongin E, Murphy SD, O'Brochta DA, Pfannkoch C, Qi R, Regier MA, Remington K, Shao H, Sharakhova MV, Sitter CD, Shetty J, Smith TJ, Strong R, Sun J, Thomasova D, Ton LQ, Topalis P, Tu Z, Unger MF, Walenz B, Wang A, Wang J, Wang M, Wang X, Woodford KJ, Wortman JR, Wu M, Yao A, Zdobnov EM, Zhang H, Zhao Q, Zhao S, Zhu SC, Zhimulev I, Coluzzi M, della Torre A, Roth CW, Louis C, Kalush F, Mural RJ, Myers EW, Adams MD, Smith HO, Broder S, Gardner MJ, Fraser CM, Birney E, Bork P, Brey PT, Venter JC, Weissenbach J, Kafatos FC, Collins FH, Hoffman SL. The genome sequence of the malaria mosquito Anopheles gambiae. Science. 2002 Oct 4;298(5591):129-49.

Ikeda SR, Soler F, Zuhlke RD, Joho RH, and Lewis DL. Heterologous expression of the human potassium channel Kv2.1 in clonal mammalian cells by direct cytoplasmic microinjection of cRNA. *Pflugers Arch* 422 :201-203, 1992.

International Human Genome Sequencing Consortium. Initial sequencing and analysis of the human genome. *Nature* 409:860-921, 2001.

Jegla T, and Salkoff L. A novel subunit for shal K+ channels radically alters activation and inactivation. *J Neurosci* 17:32-44, 1997.

Kent WJ and Haussler D. Assembly of the working draft of the human genome with GigAssembler. *Genome Research* 11:1541-1548, 2001.

Kumar S, Tamura K, Jakobsen IB, and Nei M. MEGA2: Molecular Evolutionary Genetics Analysis software. *Bioinformatics* 17:1244-1245, 2001.

Kuzhikandathil EV and Oxford GS. Dominant-negative mutants identify a role for GIRK channels in D3 dopamine receptor-mediated regulation of spontaneous secretory activity. *J. Gen. Physiol* 115:697-706, 2000.

London B, Trudeau MC, Newton KP, Beyer AK, Copeland NG, Gilbert DJ, Jenkins NA., Satler CA, and Robertson GA. Two isoforms of the mouse ether-à-go-go-related gene coassemble to form channels with properties similar to the rapidly activating component of the cardiac delayed rectifier K+ current. *Circ Res* 81:870-878, 1997.

Ludwig J, Terlau H, Wunder F, Bruggemann A, Pardo LA, Marquardt A, Stuhmer W, and Pongs O. Functional expression of a rat homologue of the voltage gated either a go-go potassium channel reveals differences in selectivity and activation kinetics between the Drosophila channel and its mammalian counterpart. *EMBO Journal* 13: 4451-4458, 1994.

Miyaka A, Mochizuki S, Yokoi H, Kohda M, and Furuichi K. New Ether-à-go-go K+ channel family members localized in human telencephelon. *J Biol Chem*, 274:25080-25025, 1999.

Morais Cabral JH, Lee A, Cohen SL, Chait BT, Li M, and Mackinnon R. Crystal structure and functional analysis of the HERG potassium channel N terminus: a eukaryotic PAS domain. *Cell* 95: 649-655, 1998.

Occhiodoro T, Bernheim L, Liu JH, Bijlenga P, Sinnreich M, Bader CR, Fischer-Lougheed J. Cloning of a human ether-à-gо go potassium channel expressed in myoblasts at the onset of fusion. *FEBS Letters* 434: 177-182, 1998.

Papazian DM, Schwarz TL, Tempel BL, Jan YN, and Jan LY. Cloning of genomic and complementary DNA from Shaker, a putative potassium channel gene from Drosophila. *Science* 237: 749-753, 1987.

Reiner DJ, Newton EM, Tian H, and Thomas JH. Diverse behavioural defects caused by mutations in Caenorhabditis elegans unc-43 CaM kinase II. *Nature* 402: 199-203, 1999.

Roberston GA, Warmke JW, and Ganetsky B. Potassium currents expressed from Drosophila and mouse eag in Xenopus oocytes. *Neuropharmacology* 35: 841-850, 1996.

Saganich MJ, Vega-Saenz de Miera E, Nadal MS, Baker H, Coetzee WA, and Rudy B. Cloning of components of a novel subthreshold-activating K+ channel with a unique pattern of expression in the cerebral cortex. *J Neurosci* 19: 10789-10802, 1999.

Saganich MJ, Machado E, and Rudy B. Differential expression of genes encoding subthreshold-operating voltage-gated K+ channels in brain. *J Neurosci* 21: 4609-4624, 2001.

Santoro B, and Tibbs GR. The HCN gene family: molecular basis of the hyperpolarization-activated pacemaker channels. *Ann New York Acad Sci* 868: 741-764, 1999.

Shi W, Wymore RS, Wang HS, Pan Z, Cohen IS, McKinnon D, and Dixon JE. Identification of two nervous system-specific members of the erg potassium channel gene family. *J Neurosci* 17 : 9423-9432, 1997.

Shi W, Wang H-S, Pan Z, Wymore RS, Cohen IS, McKinnon D, and Dixon JE. Cloning of a mammalian elk potassium channel gene and EAG mRNA distribution in rat sympathetic ganglia. *J Physiol* 511: 675-682, 1998.

Titus SA, Warmke JW, and Ganetzky B. The Drosophila erg K+ channel polypeptide is encoded by the seizure locus. *J Neurosci* 17: 875-881, 1997.

Trudeau MC, Titus SA, Branchaw JL, Ganetzky B, and Robertson GA. Functional analysis of a mouse brain Elk-type K+ channel. *J Neurosci* 19 : 2906-2918, 1999.

Trudeau MC, Warmke JW, Ganatzky B and Robertson GA. HERG, a human inward rectifier in the voltage-gated potassium channel family. *Science* 269 : 92-95, 1995.

Waldmann R, Bassilana F, de Weille J, Champigny G, Heurteaux C, and Lazdunski, M. Molecular cloning of a non-inactivating proton-gated Na+ channel specific for sensory neurons. *J Biol Chem* 272: 20975-20978, 1997.

Wang H-S, Pan Z, Shi W, Brown BS, Wymore RS, Cohen IS, Dixon JE, and McKinnon D. KCNQ2 and KCNQ3 potassium channel subunits: Molecular correlates of the M-channel. *Science* 282: 1890-1893, 1998.

Warmke J, Drysdale R, and Ganetzky B. A distinct potassium channel polypeptide encoded by the Drosophila eag locus. *Science* 252 : 1560-1562, 1991.

Warmke J, and Ganetzky B. A family of potassium channel genes related to eag in Drosophila and mammals. *Proc Natl Acad Sci U. S A.* 91: 3438-3442, 1994.

Waterston RH, Lindblad-Toh K, Birney E, Rogers J, Abril JF, Agarwal P, Agarwala R, Ainscough R, Alexandersson M, An P, Antonarakis SE, Attwood J, Baertsch R, Bailey J, Barlow K, Beck S, Berry E, Birren B, Bloom T, Bork P, Botcherby M, Bray N, Brent MR, Brown DG, Brown SD, Bult C, Burton J, Butler J,

Campbell RD, Carninci P, Cawley S, Chiaromonte F, Chinwalla AT, Church DM, Clamp M, Clee C, Collins FS, Cook LL, Copley RR, Coulson A, Couronne O, Cuff J, Curwen V, Cutts T, Daly M, David R, Davies J, Delehaunty KD, Deri J, Dermitzakis ET, Dewey C, Dickens NJ, Diekhans M, Dodge S, Dubchak I, Dunn DM, Eddy SR, Elnitski L, Emes RD, Eswara P, Eyras E, Felsenfeld A, Fewell GA, Flicek P, Foley K, Frankel WN, Fulton LA, Fulton RS, Furey TS, Gage D, Gibbs RA, Glusman G, Gnerre S, Goldman N, Goodstadt L, Grafham D, Graves TA, Green ED, Gregory S, Guigo R, Guyer M, Hardison RC, Haussler D, Hayashizaki Y, Hillier LW, Hinrichs A, Hlavina W, Holzer T, Hsu F, Hua A, Hubbard T, Hunt A, Jackson I, Jaffe DB, Johnson LS, Jones M, Jones TA, Joy A, Kamal M, Karlsson EK, Karolchik D, Kasprzyk A, Kawai J, Keibler E, Kells C, Kent WJ, Kirby A, Kolbe DL, Korf I, Kucherlapati RS, Kulbokas EJ, Kulp D, Landers T, Leger JP, Leonard S, Letunic I, Levine R, Li J, Li M, Lloyd C, Lucas S, Ma B, Maglott DR, Mardis ER, Matthews L, Mauceli E, Mayer JH, McCarthy M, McCombie WR, McLaren S, McLay K, McPherson JD, Meldrim J, Meredith B, Mesirov JP, Miller W, Miner TL, Mongin E, Montgomery KT, Morgan M, Mott R, Mullikin JC, Muzny DM, Nash WE, Nelson JO, Nhan MN, Nicol R, Ning Z, Nusbaum C, O'Connor MJ, Okazaki Y, Oliver K, Overton-Larty E, Pachter L, Parra G, Pepin KH, Peterson J, Pevzner P, Plumb R, Pohl CS, Poliakov A, Ponce TC, Ponting CP, Potter S, Quail M, Reymond A, Roe BA, Roskin KM, Rubin EM, Rust AG, Santos R, Sapojnikov V, Schultz B, Schultz J, Schwartz MS, Schwartz S, Scott C, Seaman S, Searle S, Sharpe T, Sheridan A, Shownkeen R, Sims S, Singer JB, Slater G, Smit A, Smith DR, Spencer B, Stabenau A, Stange-Thomann N, Sugnet C, Suyama M, Tesler G, Thompson J, Torrents D, Trevaskis E, Tromp J, Ucla C, Ureta-Vidal A, Vinson JP, Von Niederhausern AC, Wade CM, Wall M, Weber RJ, Weiss RB, Wendl MC, West AP, Wetterstrand K, Wheeler R, Whelan S, Wierzbowski J, Willey D, Williams S, Wilson RK, Winter E, Worley KC, Wyman D, Yang S, Yang SP, Zdobnov EM, Zody MC, Lander ES. Initial sequencing and comparative analysis of the mouse genome. Nature. 2002 Dec 5;420(6915):520-62.

Wei A, Covarrubias M, Butler A, Baker K, Pak M, and Salkoff L. K+ current diversity is produced by an extended gene family conserved in Drosophila and mouse. *Science* 248: 599-603, 1990.

Weinshenker D, Wei A, Salkoff L, and Thomas JH. Block of an ether-à-go-gɵ like K+ channel by imipramine rescues egl-2 excitation defects in Caenorhabditis elegans. *J Neurosci* 19 : 9831-9840, 1999.

Wimmers S, Wulfsen I, Bauer CK, Schwarz JR. Erg1, erg2 and erg3 K channel subunits are able to form heteromultimers. Pflugers Arch 2001 Jan;441(4):450-5

Figure Legends

Figure 1. Alignment of the deduced amino acid sequences of human KCNH8, rat Kcnh8, human KCNH3 and human KCNH4. Amino acid positions are given at the right margin and identical residues are shaded. Dashes indicate gaps in the alignment. Transmembrane domains S1-S6 are underlined with a solid black line and the potassium channel pore motif is underlined with a solid gray line. An N terminal PAS domain (small dashes) and a cyclic nucleotide binding domain (long dashes) are also underlined. The sources of the rat Kcnh8, human KCNH4 and human KCNH3 sequences are Genbank accession numbers AF061957, BA83590 and BA83592, respectively.

Figure 1

Figure 2. Phylogenetic tree of the Eag gene family. Gene names are given at the right of terminal branches and prefix indicates species (cb = *Caenorhabditis briggsae*; ce = *Caenorhabditis elegans*; dm =*Drosophila melanogaster* ; ag = Anopheles gambiae; h = human; m = mouse; r = rat). Colors indicate phylogenetic groups (mammals = red; insects = green; worms = blue). Branch lengths indicate the relative degree of divergence and numbers indicate the % occurrence of the branch point in bootstrap tests of the phylogeny. The tree was constructed using the minimum evolution algorithm in MEGA2.1.

Figure 2

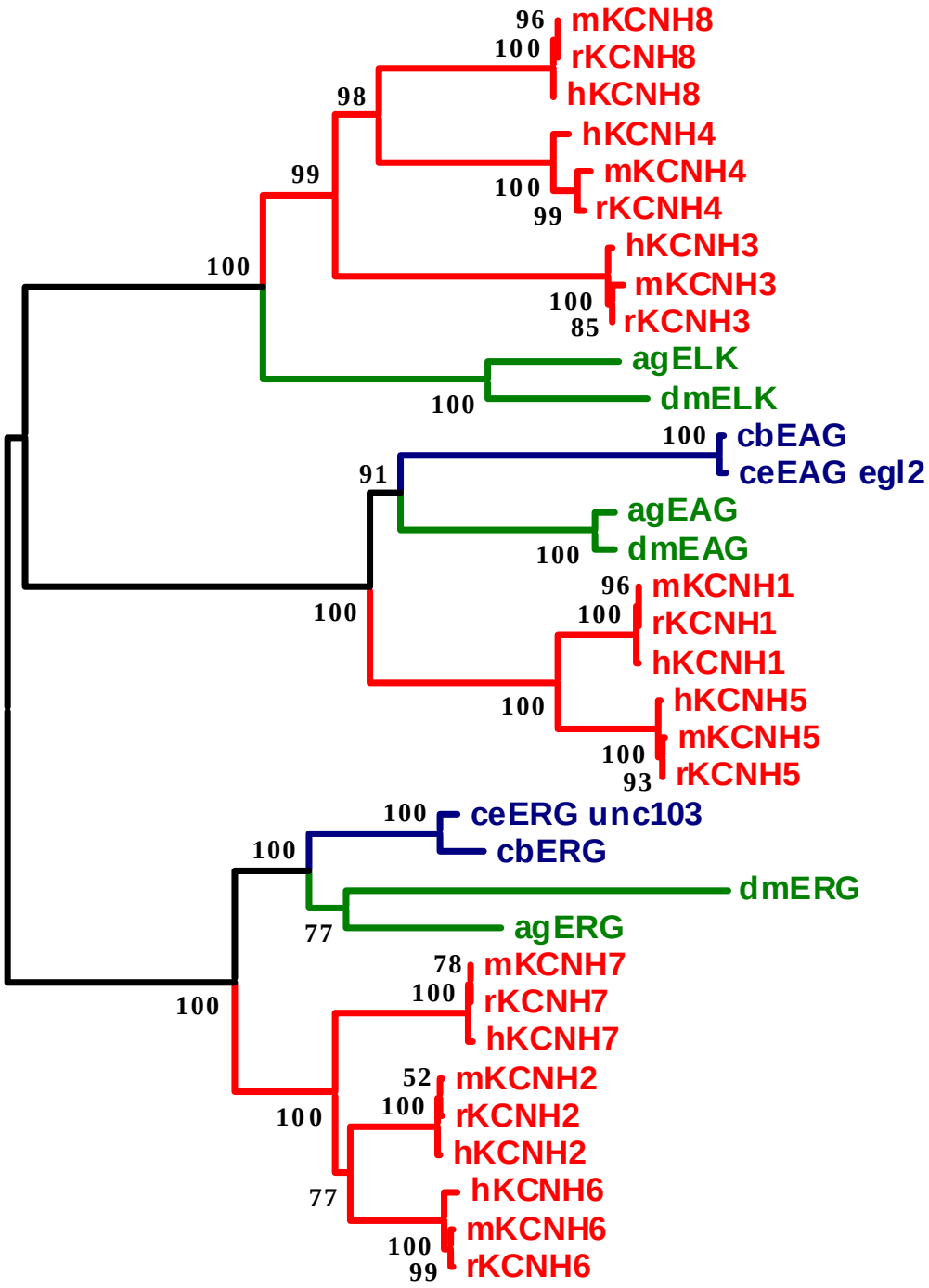
96
100
mKCNH8
rKCNH8
hKCNH8
98
hKCNH4
99
mKCNH4
100
99
rKCNH4
hKCNH3
100
mKCNH3
100
85
rKCNH3
agELK
100
dmELK
100
cbEAG
91
ceEAG egl2
agEAG
100
dmEAG
96
mKCNH1
100
100
rKCNH1
hKCNH1
100
hKCNH5
mKCNH5
100
93
rKCNH5
100
ceERG unc103
100
cbERG
dmERG
77
agERG
78
mKCNH7
100
rKCNH7
hKCNH7
100
52
mKCNH2
100
rKCNH2
hKCNH2
77
hKCNH6
mKCNH6
100
99
rKCNH6

Figure 3. Expression patterns of human Elk family genes in the nervous system as determined by real time quantitative PCR. (a) human KCNH8, (b) human KCNH3, (c) human KCNH4. Tissues for the RNA samples were identical for each gene and are given at the bottom of C. Values are reported as a percentage of the expression level of the ribosomal protein RS9, a housekeeping gene. Percentages were calculated based on determinations of copy number for each gene as discussed in the Methods section.

Figure 3

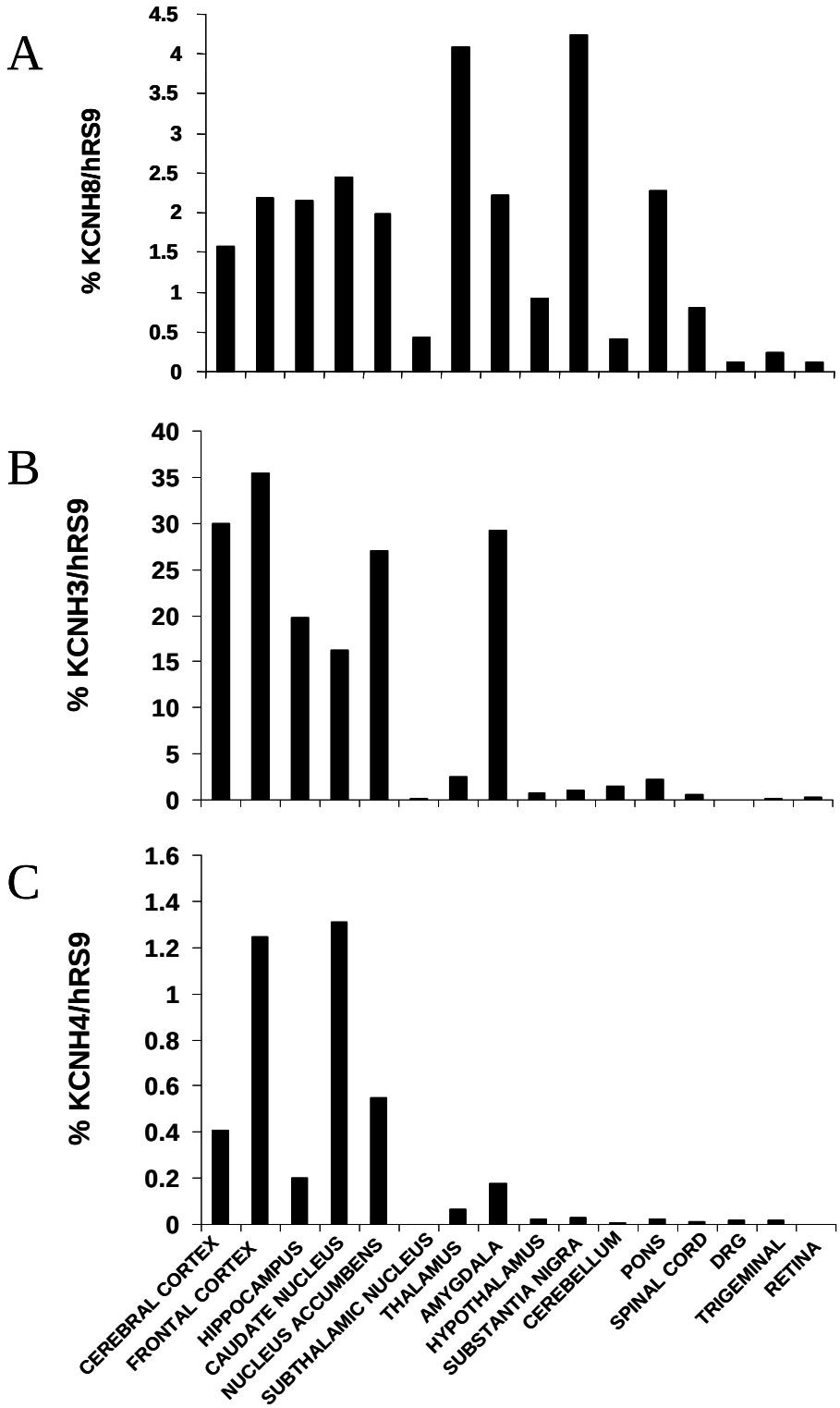
A
% KCNH8/hRS9
4.5
4
3.5
3
2.5
2
1.5
1
0.5
0
B
% KCNH3/hRS9
40
35
30
25
20
15
10
5
0
C
% KCNH4/hRS9
1.6
1.4
1.2
1
0.8
0.6
0.4
0.2
0
CEREBRAL CORTEX
FRONTAL CORTEX
HIPPOCAMPUS
CAUDATE NUCLEUS
NUCLEUS ACCUMBENS
SUBTHALAMIC NUCLEUS
THALAMUS
AMYGDALA
HYPOTHALAMUS
SUBSTANTIA NIGRA
CEREBELLUM
PONS
SPINAL CORD
DRG
TRIGEMINAL
RETINA

Figure 4. Characterization of human KCNH8 in *Xenopus* oocytes. Representative two-electrode whole-cell voltage clamp recordings from a *Xenopus* oocyte injected with KCNH8 cRNA. Currents were elicited with a series of 3 s depolarizing steps (-100 mV to +10 mV in 10 mV increments) from a holding potential of -100 mV in regular ND96 (A) and hi-K^+ ND96 (B). C) Activation curve for KCNH8 expressed in *Xenopus* oocytes. Average normalized tail current amplitude at –60 mV from 10 oocytes in normal ND96 (circles) and 8 oocytes in hi-K^+ ND96 (squares) are plotted against the step potential. Half-maximal activation of KCNH8 occurred at –62.4mV ± 1.2 mV in regular ND96 and -68.0 ± 1.2mV in hi-K^+ ND96. D) KCNH8 reversal potentials. Reversal potentials were calculated from linear fits of instantaneous tail currents (see methods) against repolarization potential in normal and hi-K^+ ND96. Reversal potentials (symbols) were plotted against the extracellular K^+ concentration and fitted with a logarithmic regression (solid line), yielding a slope of 48 mV per decade. The dashed line represents the relation for a purely potassium selective channel with a slope of 58mV per decade (assuming an intracellular K^+ concentration of 100mM). E) Average slow activation time constants and F) average fast activation time constants from oocytes injected with KCNH8 cRNA. Average slow and fast deactivation time constants are plotted against tail current potential in E and F, respectively. The horizontal lines in A and B represent 0μA.

Figure 4

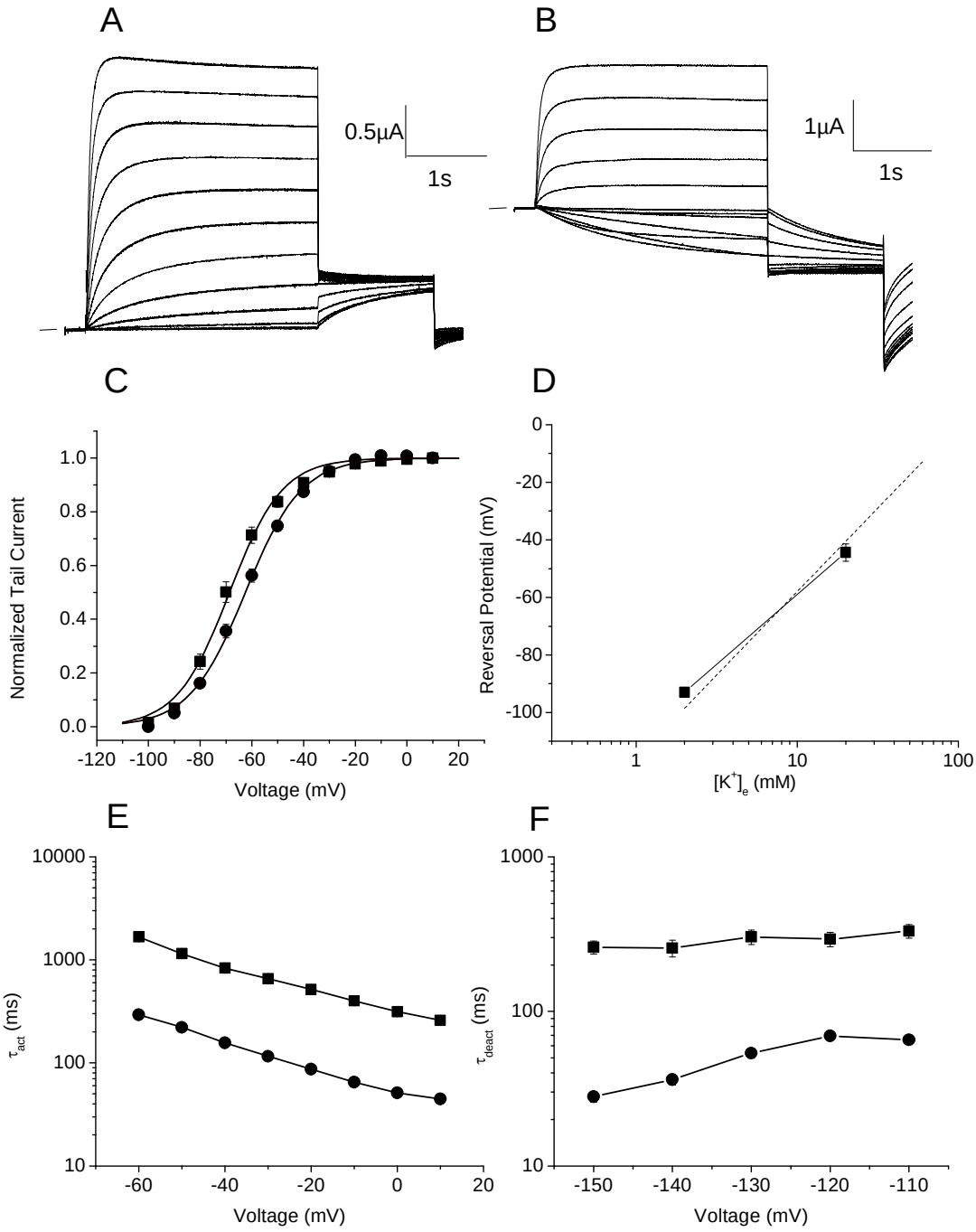
A
0.5μA
1s
B
1μA
1s
C
Normalized Tail Current
Voltage (mV)
D
Reversal Potential (mV)
[K+]e (mM)
E
τact (ms)
Voltage (mV)
F
τdeact (ms)
Voltage (mV)

Figure 5. Human KCNH8, KCNH3 and KCNH4 dominant negative constructs depress KCNH8 expression. Representative two electrode voltage-clamp recordings from *Xenopus* oocytes injected with human KCNH8 alone (A), KCNH8 and KCNH8 DN (B), KCNH8 and KCNH3 DN (C) or KCNH8 and KCNH4 DN (D). To elicit KCNH8 currents, oocytes were depolarized to +40 mV for 3s, and repolarized to –60mV for 1s, from a holding potential of –100mV. E) Current-voltage relationships were constructed for KCNH8 in the absence (■) or presence of KCNH8 DN (▲),KCNH3-DN (▼) or KCNH4-DN (●). Symbols represent the mean (S.E.M) current amplitude of 8 - 10 oocytes per group. The horizontal lines in A – D represent 0μA.

Figure 5

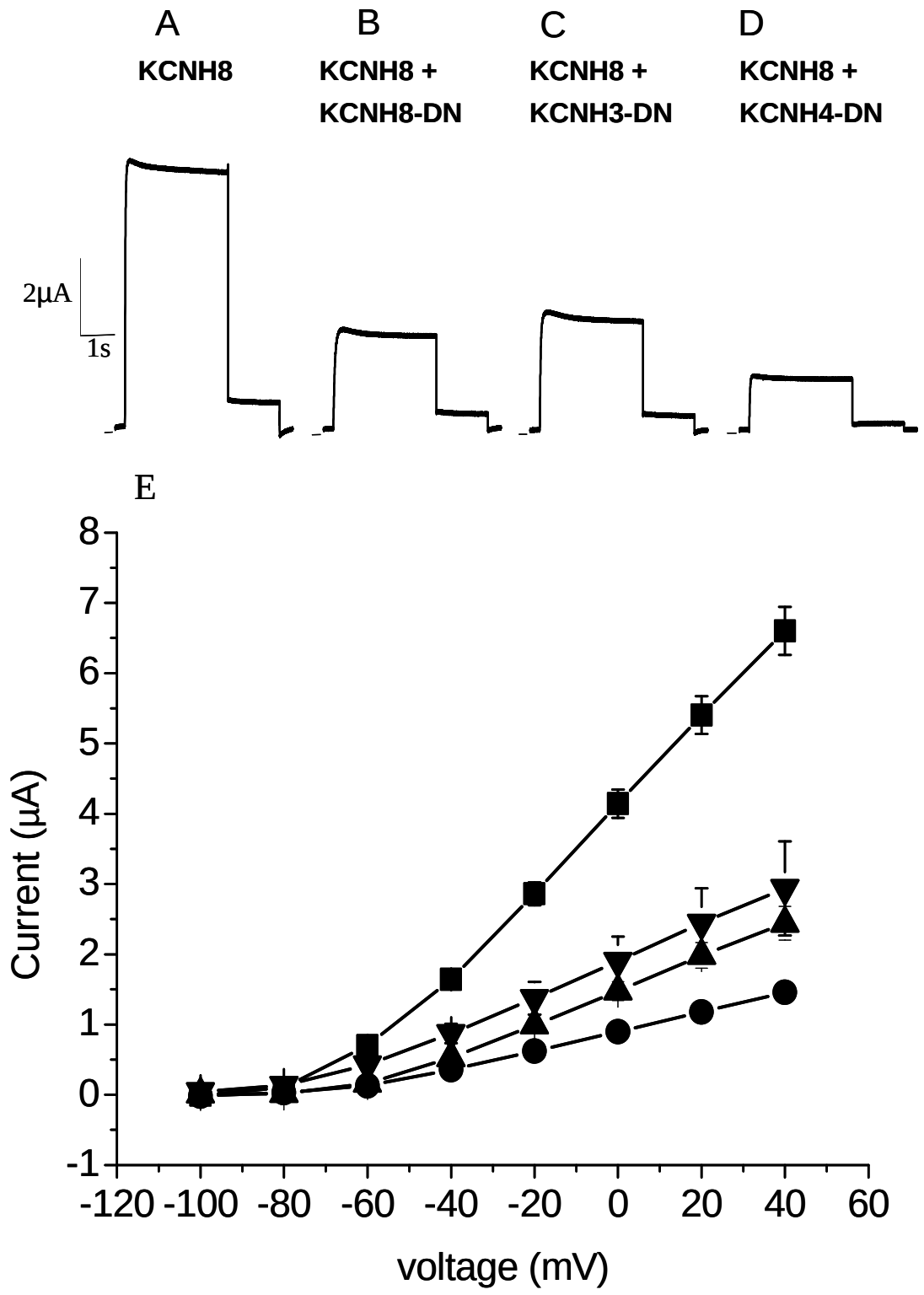
A
KCNH8
B
KCNH8 +
KCNH8-DN
C
KCNH8 +
KCNH3-DN
D
KCNH8 +
KCNH4-DN
2µA
1s
E
Current (µA)
voltage (mV)
8
7
6
5
4
3
2
1
0
-1
-120
-100
-80
-60
-40
-20
0
20
40
60

Figure 6. Human Elk dominant negative constructs do not affect KCNH5 (hEag2), KCNH7 (hErg3) or KCNB1 (hKv2.1) expression. A) Current-voltage relationships for KCNH5 alone (■) or in the presence of KCNH3-DN (●) or KCNH4-DN (▲). B) Current-voltage relationships for KCNH7 alone (■) or in the presence of KCNH8-DN (▼) or KCNH3-DN (●). C) Current-voltage relationships for KCNB1 alone (■) or in the presence of KCNH8-DN (▼), KCNH3-DN (●) or KCNH4-DN (▲). Symbols represent the mean (S.E.M) current amplitude of 8 - 13 oocytes per group.

Figure 6

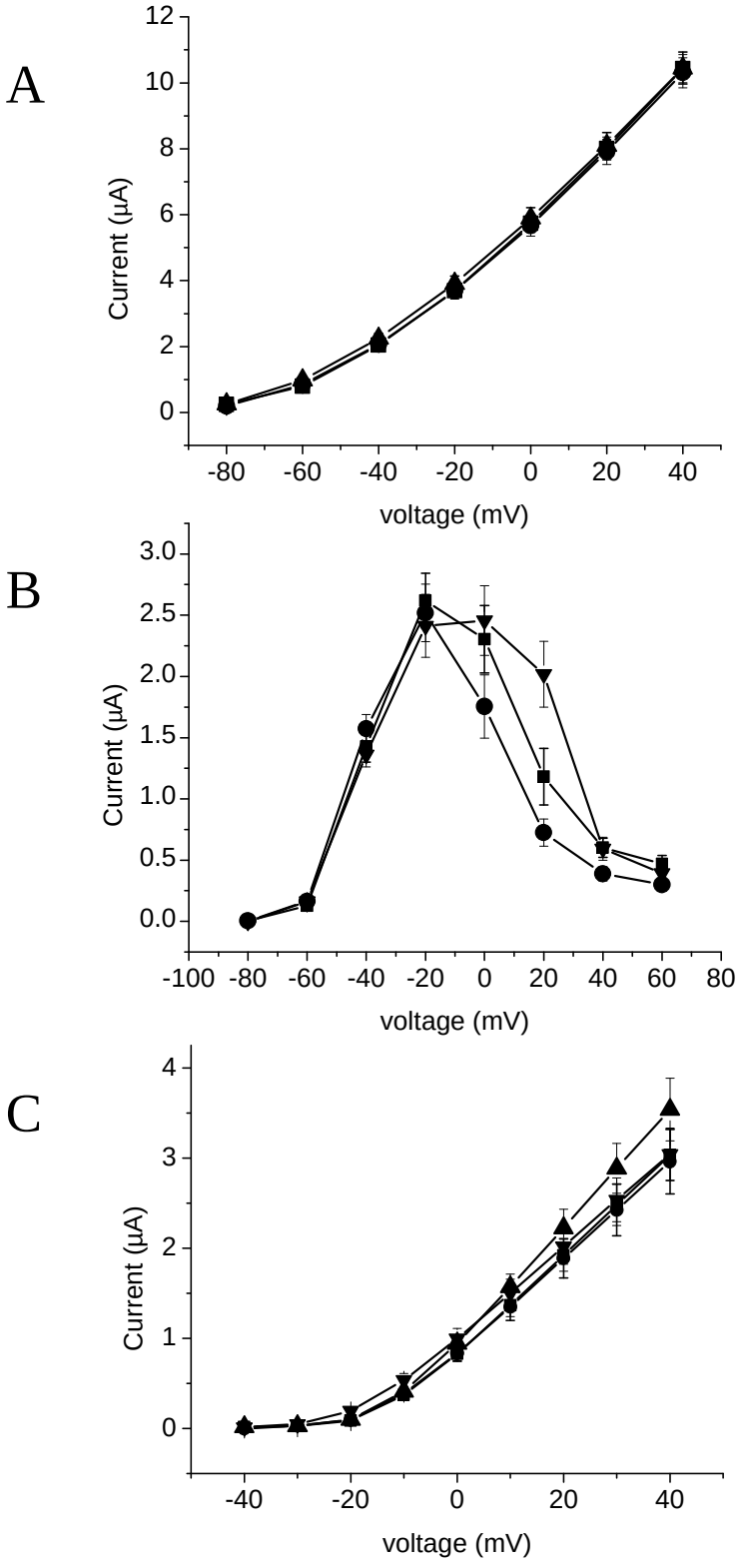
A
Current (μA)
voltage (mV)
B
Current (μA)
voltage (mV)
C
Current (μA)
voltage (mV)